Active OB stars: structure, evolution, mass loss, and critical limits
Proceedings IAU Symposium No. 272, 2010
C. Neiner, G. Wade, G. Meynet & G. Peters, eds.

doi:10.1017/S1743921311011082

Pulsations in Wolf-Rayet stars: observations with MOST

André-Nicolas Chené[1,2] and Anthony F. J. Moffat[3,4]

[1]Departamento de Física, Universidad de Concepción, Casilla 160-C, Concepción, Chile
email: achene@astro-udec.cl

[2]National Research Council of Canada, Herzberg Institute of Astrophysics,
5071, West Saanich Road,Victoria (BC), V9E 2E7

[3]Département de Physique, Université de Montréal,
C. P. 6128, succ. centre-ville, Montréal (Qc) H3C 3J7

[4]Centre de Recherche en Astrophysique du Québec, Canada
email: moffat@astro.umontreal.ca

Abstract. Photometry of Wolf-Rayet (WR) stars obtained with the first Canadian space telescope *MOST* (Microvariability and Oscillations of STars) has revealed multimode oscillations mainly in continuum light that suggest stellar pulsations could be a significant contributing factor to the mass-loss rates. Since the first clear detection of a pulsation period of P = 9.8h in WR123, two other stars have also shown periods of a few days, which must be related to stellar pulsations.

Keywords. stars: Wolf-Rayet, stars: oscillations (including pulsations), stars: winds, outflows

1. Introduction

The wind momentum (dM/dtv) of the Wolf-Rayet (WR) stars is a factor 10 times higher than the radiative momentum outflow rate (L/c); radiation pressure doesnt seem to be sufficient to initiate the strong winds. Hence, another driving mechanism should be present near, or at the surface of the star. Theoretical work suggest that strange-mode pulsations (SMPs) are present in the envelope of hot and luminous stars with a large luminosity-to-mass ratio, where the thermal timescale is short compared to the dynamical timescale, and where radiation pressure dominates (Glatzel *et al.* 1993). Hence, the most violent SMPs are expected in classical WR stars, where SMPs manifest themselves in cyclic photometric variability with periods ranging from minutes to hours (Glatzel *et al.* 1999). However, these variability are expected to be epoch-dependent, with small amplitude, therefore, very difficult to detect from the ground.

The space telescope *MOST* (Microvariability and Oscillations of STars, Matthews *et al.* 1999, Walker *et al.* 2003) contains a 15-cm Rumak-Maksutov telescope imaging onto a CCD detector via a custom optical broadband (350-750 nm) filter. From its polar Sun-synchronous orbit of altitude 820 km and period 101 min, *MOST* has a continuous viewing zone (CVZ) about 54° wide within which it can monitor target fields for up to two months without interruption. Targets brighter than V∼6 mag are observed in Fabry imaging mode, while fainter targets (like most of the WR stars in the CVZ) are observed in direct imaging mode, similar to standard CCD photometry with a groundbased instrument. The photometry is non-differential, but given the orbit, thermal and design characteristics of *MOST*, experience has shown that it is a very photometrically stable platform even over

long timescales (with repeatability of the mean instrumental flux from a non-variable target with V∼11-12 to within about 1 mmag over a month).

2. Three First Stars Observed With *MOST*

Since its launch, *MOST* has observed one WR star per year. The first one is the famous WR 123 of the WN8 type (Lefèvre *et al.* 2005). Its light curve has a total amplitude of 10 mmag and shows variations on timescales of ∼hours to days. It displays dips which seem to occur every 14–15 days, but these features are not always identical and they were not sufficiently well monitored during the 38 days of observation. Also, the periodogram shows a significant peak at ∼ 2.45 c d^{-1} (i.e. P∼9.8 hours). Two quite different scenarios have been proposed to explain these observations. Townsend & MacDonald (2006) find that a deep, hot Fe opacity bump can lead to g-mode pulsations, while Dorfi et al. (2006) find that a cooler Fe opacity bump can produce SMPs. The latter is in contrast with Glatzel *et al.* (1993, 1999) work, where SMP periods of order 10 minutes were predicted to prevail in WR stars. The longer timescales and period found in WR 123 are most likely a result of the puffed-up nature of WN8 stars ($R_* \sim 15 R_\odot$, according to Crowther *et al.* 1995), compared to their much more compact early-type WN brethren. In these two theoretical studies, the former group assumed a traditionally small stellar radius ($R_* \sim 2 R_\odot$), while the latter group assumed significant hydrogen (X_H=0.35, compared to the observed value of 0.00. Both of these assumptions contradict what we know about this star, thus casting some doubt on their applicability.

On the second year was observed WR 103, a dust-making WR star of the Carbon sequence. No clear period could be found although the light curve shows clear variations with an amplitude of ∼5 mmag (Marchenko *et al.* 2006). Simultaneous spectroscopy has shown that the changes are coming from the continuum light, and not from the expanding wind, where the spectral emission are formed.

Finally, WR 111 (WC5) was observed in 2006. Moffat *et al.* (2008) have found no coherent Fourier components above the 50 part per million level over the whole interval for frequencies f<10 c d^{-1}. Simultaneous spectroscopic observations reveal a normal level of stochastic clumps propagating in the wind, which has no effect on period detection.

3. WR 124

WR 124 = 209BAC = QR Sge = Merrill's star is a moderately bright (v = 11.08, $b-v$ = 1.07), reddened (A_v = 4.43 mag), northern [RA(2000) = 19:11:30.88, DEC(2000) = +16:51:38.2] Galactic (l = 50.198°, b = +3.310°) WR star in the cool-nitrogen sequence with type WN8h (Smith *et al.* 1996). Located at a distance of 3.35 kpc (Marchenko, Moffat & Crowther, in prep.), it is a runaway star (e.g. Moffat *et al.* 1998).

Fig. 1 shows the entire *MOST* light curve of WR 124 (*upper*) and a control star (*lower*), binned for each *MOST* orbit. Although significant variations are seen on timescales longer than ∼a day, no such variations are seen on shorter timescales and binning allows one to increase the photometric point-to-point *rms* precision from ∼3 mmag before binning to ∼0.5 mmag after binning. Fig. 1 shows a time-frequency plot with straddled 8-day (double the best period) sampling. There is a family of three plausible frequencies for WR 124, but first examination of the data shows that the most probable frequency is unique, and is located at ∼0.19 c d^{-1} (P∼5.3 d). Simultaneous spectral monitoring gives a period of P∼4.45 d. The spectral line-profile variability of WR 124 is very similar to the one observed for WR 123, although with a smaller amplitude. Since both these stars are of similar spectral types, the same type of pulsation may be present in each. Also,

https://doi.org/10.1017/S1743921311011082 Published online by Cambridge University Press

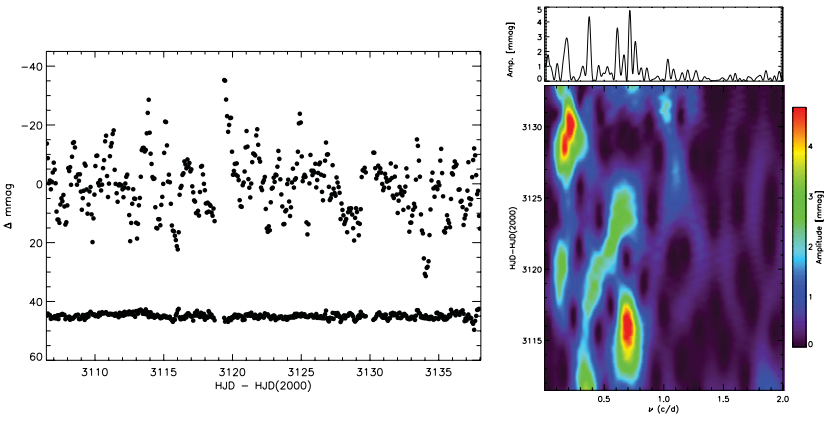

Figure 1. *Right*: *MOST* light curve of WR 124 in 101-minute MOST-orbit bins. *Left*: Fourier amplitude spectrum of the binned *MOST* light curve and Time-frequency Fourier plot with 8-day running windows in time.

from previous ground-based observations, all the ∼10 relatively well-observed WN8 stars show a similar high degree of intrinsic variability (Antokhin *et al.* 1995, Marchenko *et al.* 1998), implying that all cool WR stars may show similar behavior.

4. WR 110

WR 110 is a moderately bright ($v = 10.30$, $b - v = 0.75$), reddened ($A_v = 3.83$ mag), southern [RA(2000) = 18:07:56.96, DEC(2000) = -19:23:56.8] Galactic (l = 10.80^o, b = $+0.39^o$) WR star in the mid-nitrogen sequence with type WN5-6b (Smith *et al.* 1996). Although to date it lacks any obvious binary signature, a comprehensive radial velocity search has not yet been carried out. However, WR 110 does have relatively high X-ray flux, with a significant hard component above 3 keV, compared to its lower-energy 0.5 keV emission, as seen in most WN stars (Skinner *et al.* 2002). The lower-energy component likely arises due to small-scale turbulent shocks in the wind, with velocity dispersion ∼100 km s^{-1}, as seen in virtually all WR-star winds (Lépine & Moffat 1999) and other luminous hot stars (e.g. Eversberg *et al.* 1998, Lépine & Moffat 2008. The former hard component implies velocities of at least 10^3 km s^{-1}, which are more difficult to explain, without invoking an additional mechanism to provide such high speeds (e.g. accretion onto a low-mass companion or colliding winds with a massive companion). However, WR 110 emits normal thermal radio emission from its wind (Skinner *et al.* 2002), which lends little support for its binary nature.

Recently St-Louis *et al.* (2009) have examined a northern sample of 25 WR stars for the presence of Corotating-Interaction Regions (CIRs) via large-scale variations exhibited on broad, strong emission lines. Some 20% of these stars show clear signatures of such effects, with WR 110 situated at the limit between those stars that show CIRs and those that do not. In addition, some (and possibly all, given the limited number of spectra) stars in the sample unsurprisingly show small-scale wind-clump variations. As we show in this investigation, it is possible and even likely, that WR 110's hard X-rays arise in the shocks produced by its CIRs rotating at velocities of $\sim 10^3$ km s^{-1} relative to the ambient wind.

Fig. 2 shows the entire *MOST* light curve of WR 110 (*upper*) and a control star (*lower*), binned for each *MOST* orbit. Fig 2 also shows the Fourier spectrum for the *MOST* photometry. Here we see that the most significant peak occurs at a frequency of $\nu_0 = 0.245\ cd^{-1}$ (P = 4.08 d), with harmonics of this frequency at, or close to, $n \times \nu_0$, with

https://doi.org/10.1017/S1743921311011082 Published online by Cambridge University Press

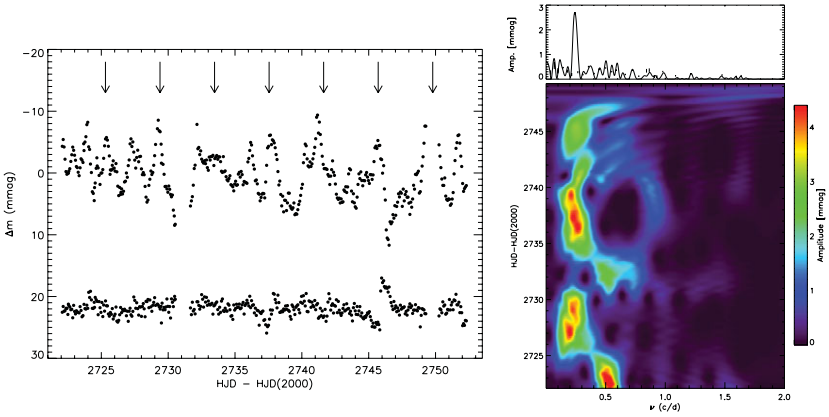

Figure 2. *Right*: *MOST* light curve of WR 110 in 101-minute MOST-orbit bins. The vertical lines indicate intervals of period 4.08 d starting at t_0 = HJD 2454270.31. *Left-Top*: Fourier amplitude spectrum of the binned *MOST* light curve. The highest peak refers to the adopted fundamental frequency corresponding to a period of P = 4.08 d. Harmonics are indicated at frequencies at multiples of 2 through 6 times fundamental. *Left-Bottom* : Time-frequency Fourier plot with 8-day running windows in time.

n = 2, 3, 4, 5 and 6. A few other peaks do occur at lower relative amplitudes, notably at periods longer than ∼a day, but with no obvious order or interrelationship. No significant peaks occur at longer than a day. We assume that all this implies one dominating (non-sinusoidal) periodicity with P = 4.08d, plus mainly stochastic noise (probably related to wind clump activity) on timescales longer than a day. Examination of the light curve in Fig. 2 shows relatively sharp cusps occurring on this time scale (i.e. P = 4.08 d, starting at t_0 = HJD 2 454 270.27) in all seven cases but one (the third case), although even then there is a rise in brightness, though not cusp-like. The cusps have typical widths at the base of ∼ a day. Such cusps are clearly non sinusoidal, requiring a series of successive harmonics to reproduce them, as observed. Fig. 2 also shows a time-frequency plot with straddled 8-day (double the best period) sampling. This plot reveals that the 4.08-day period stands out at all times except just before the middle of the run and at the ends (where edge effects come into play). The former is compatible with the apparently suppressed third cusp, as noted above.

The most likely scenario to explain the low-amplitude (∼1 %) 4.08 d periodicity and cusp-like behavior in the *MOST* light curve, along with mostly unrelated spectral variations, appears to be large-scale, emitting over-density structure rotating with the wind. An attractive scenario for this are the CIRs (or their source at the base of the wind) proposed for O star winds by Cranmer & Owocki (1996). We now apply this idea to WR 110 in the following way.

First, we assume that the CIRs are continuum-emitting thermal sources, heated by the associated shock action created by a hot spot on the underlying rotating star with the ambient wind. Most of their emission must arise close to the star, where the ambient wind density is highest, as inspired by the simulations of Cranmer & Owocki (1996). Alternatively, the emission could arise in a hot spot at or close to the stellar surface, that produces the CIR. To simplify our calculations, we assume a point source located at some radius $R_s = \gamma R_*$ from the center of the star, with $\gamma > 1$ and R_* being the stellar core radius. For simplicity (and following Cranmer & Owocki 1996) we assume the CIR to initiate at the stellar rotation equator.

https://doi.org/10.1017/S1743921311011082 Published online by Cambridge University Press

In this scenario, the changes in the light-curve are caused by the assumed CIR-associated point source attenuated by the wind and seen at different angles with the line of sight as it rotates on the near side of the WR star. In this study, we use a simple WR wind model derived by Lamontagne *et al.* (1996) in the context of wind eclipses for WR + O systems. Hence, the change in magnitudes is defined as :

$$\Delta m \, = \, constant \, - \, 2.5 \log_{10} \left(I_{WR} + I_s \mathrm{e}^{-\tau} \right), \tag{4.1}$$

with arbitrary constant and where I_{WR} is the intensity of the WR star and I_s, the intensity of the hot spot. Here the total opacity τ between the source and the observer, passing through the WR wind is :

$$\tau = k \int_{z_0}^{\infty} d\left(z/R_s\right) \left[r^2 \left(1 - R_*/r\right)^{\beta} \right]^{-1} \tag{4.2}$$

where $z_0 = -(R_s \sin i) \cos 2\pi\phi$, with R_s, the radial position of the hot spot (or the region of light emission) and i, the inclination of the rotation axis relative to the observer. We allow for a WR wind with a β law, in which the actual β value will be fitted. Since the CIR source is much closer to the inner WR wind than the O star is in the (non photospheric eclipsing) binary case, we expect that $\beta = 0$ will not be a good choice, as it was in the case of WR + O binaries. Following Skinner *et al.* (2002), a radio-based thermal mass-loss rate for the WR star of $\dot{M} = 1.6\ 10^{-5} M_{\odot}\, yr^{-1}$, after dividing by a factor three to allow for wind clumping; taking wind terminal speed of v_{∞} =2100 km s^{-1}; and assuming a WR core radius $R_* = 4R_{\odot}$, we find an opacity constant as in Lamontagne *et al.* (1996) $k = \alpha\sigma_e/[4\pi m_p v_{\infty} R_s] = 0.0028/\gamma$. In our case, we are primarily interested in the phases centered at phase 0.50 (i.e. when the source is between the star and the observer) since, normally, the CIR point source will not be visible as it rotates on the back side of the WR star.

We calculated the Equation 4.1 numerically, centered at phase 0.5 for half a rotation period, as a function of the parameters β, I_s/I_{WR}, i, and γ. We consider two cases: (a) an optically thin point source, whose emission is isotropic in direction, and (b) and an optically thick source whose emission is maximum when seen perpendicularly to the stellar surface, dropping to zero when seen parallel to the surface (i.e. like pancakes on or near the stellar surface). In case (a) we have the light curve excess from the hot spot and in case (b), we have to multiply the net spot intensity (I_s) from Equation 4.1 by the projection factor $(\sin i) cos[2\pi(\phi - 0.5)]$.

Taking the second cusp in Fig. 2 as the cleanest, most representative form of the hotspot light curve, we fit the above parameters to match the data best, for i = 90° (to give the maximum effect). In case (b), the values of γ and β, which are always strongly coupled (since an increase in γ making the hotspot source further away from the star, has to be compensated for by an increase in absorbing material at larger distances, i.e. an increased β value, in order to reproduce best the observed light-curve cusps), tend to be slightly smaller than in case (a), since the projection factor in case (b) already provides a start (but only a start) to the correct form for the cuspy light curve, that requires less extended wind opacity to bring about the observed cuspy shape. Indeed, it is the varying opacity through the WR wind as the WR star rotates, which leads to the cuspy shape; the closer the source is to the stellar surface (i.e. γ closer to unity), the smaller the β value (and less extended the wind) necessary to give the cuspy shape. All the best solutions for the thin and the thick cases are plotted in Fig. 3.

https://doi.org/10.1017/S1743921311011082 Published online by Cambridge University Press

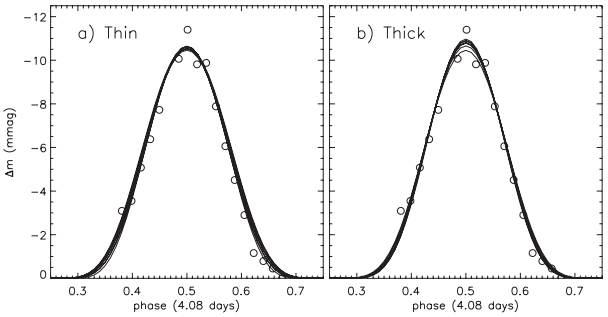

Figure 3. The data points refer to the second cusp indicated by a vertical line in Fig. 2. The curves indicate the best fits for (a) an optically thin point source and (b) an optically thick source (see text).

References

Antokhin, I., Bertrand, J.-F., Lamontagne, R., & Moffat, A. F. J. *et al.* 1995, *AJ*, 109, 817
Cranmer, S. R. & Owocki, S. P. 1996, *ApJ*, 462, 469
Crowther, P. A., Hillier, D. J., & Smith, L. J. 1995, *A&A*, 293, 403
Dorfi, E. A., Gautschy, A., & Saio, H. 2006, *A&A*, 453, L35
Eversberg, T., Lepine, S., & Moffat, A. F. J. 1998, *ApJ*, 494, 799
Glatzel, W., Kiriakidis, M., Chernigovskij, S., & Fricke, K. J. 1999, *MNRAS*, 303, 116
Glatzel, W., Kiriakidis, M., & Fricke, K. J. 1993, *MNRAS*, 262, L7
Lamontagne, R., Moffat, A. F. J., Drissen, L., & Robert, C. *et al.* 1996, *AJ*, 112, 2227
Lefèvre, L., Marchenko, S. V., Moffat, A. F. J., Chené, A. N. *et al.* 2005, *ApJ* (Letters), 634L, 109
Lépine, S. & Moffat, A. F. J. 1999, *ApJ*, 514, 909
Lépine, S. & Moffat, A. F. J. 2008, *AJ*, 136, 548
Matthews, J., Kuschnig, R., Walker, G., & Johnson, R. *et al.* 1999, *JRASC*, 93, 183
Marchenko, S. V., Moffat, A. F. J., Eversberg, T., & Morel, T. *et al.* 1998, *MNRAS*, 294, 642
Marchenko, S., Lefevre, L., Moffat, A. F., & Zhilyaev, B. E. *et al.* 2006, in: *Bulletin of the American Astronomical Society*, 38, p. 121
Moffat, A. F. J., Marchenko, S. V., Bartzakos, P., & Niemela, V. S. *et al.* 1998, *ApJ*, 497, 896
Moffat, A. F. J., Marchenko, S. V., Zhilyaev, B. E., & Rowe, J. F. *et al.* 2008, *ApJ* (Letters), 679L, 45
Skinner, S. L., Zhekov, S. A., Güdel, M., & Schmutz, W. 2002, *ApJ*, 572, 477
Smith, L. F., Shara, M. M., & Moffat, A. F. J. 1996, *MNRAS*, 281, 163
St-Louis, N., Chené, A.-N., & Schnurr, O. & Nicol, M.-H. 2009, *ApJ*, 698, 1951
Townsend, R. H. D. & MacDonald, J. 2006, *MNRAS*, 368, L57
Walker, G., Matthews, J., Kuschnig, R., & Johnson, R. *et al.* 2003, *PASP*, 115, 1023

Discussion

PULSE: You have mentioned that the two theoretical studies on WR123 have assumed wether stellar radius too small (Tonwsend & MacDonald 2006), or an hydrogen abundance too high (Dorfi *et al.* 2006). Since Rich is in the auditory, he might be able to comment on this?

TOWNSEND: The stellar radius depends quite critically on the presumed hydrogen abundance. We don't see any evidence for hydrogen in WR 123. Thus, I have assumed an X_H=0 for the star, and my stellar evolution models then predict a small hydrostatic radius for the star. With this small radius, the observed MOST variability must be due to g modes rather than strange modes.

https://doi.org/10.1017/S1743921311011082 Published online by Cambridge University Press